

Electrochemical Investigation of the Synergistic Effect Between Molybdate and Tungstate on Surface Passivation of Carbon Steel

Pei Zhang^{1,*}, Yijiang Chen², Yong Zhou^{2,**}, Fuan Yan², Guochao Nie³

¹ College of Chemical and Food Science, Yulin Normal University, Yulin 537000, China

² Key Laboratory for Green Chemical Process of Ministry of Education, Wuhan Institute of Technology, Wuhan 430205, China

³ College of Physics and Telecommunication, Yulin Normal University, Yulin 537000, China

*E-mail: zhang200622072@163.com

**E-mail: zhouyong@wit.edu.cn

Received: 1 October 2020 / Accepted: 9 November 2020 / Published: 30 November 2020

The purpose of this paper was to understand the synergistic effect between molybdate and tungstate for the surface passivation of carbon steel, particularly to find the optimum ratio of molybdate and tungstate. For Q235 carbon steel in mixed Na₂MoO₄ and Na₂WO₄ solutions with different ratios of MoO₄²⁻ and WO₄²⁻, the electrochemical methods, including potentiodynamic polarization, Mott-Schottky and electrochemical impedance spectroscopy (EIS), were applied. Under the total concentration of 0.2 mmol/L, the ratio variation of MoO₄²⁻ and WO₄²⁻ did not affect the corrosion behavior of Q235 carbon steel, and the main corrosion parameters, including corrosion potential (E_c), corrosion current density (i_c), flat band potential (U_f) and inner-layer passive film resistance (R_i) were independent of the ratio variation; however, the ratio variation of MoO₄²⁻ and WO₄²⁻ affected the passivation behavior of Q235 carbon steel obviously, and the main passivation parameters, including transpassive potential (E_t), donor density (N_D) and outer-layer passive film resistance (R_o), presented the optimum level when the ratio of MoO₄²⁻ and WO₄²⁻ was one to one. At the same time, the related mechanisms of corrosion and passivation were also discussed.

Keywords: carbon steel; molybdate (MoO₄²⁻); tungstate (WO₄²⁻); surface passivation; synergistic effect; electrochemistry

1. INTRODUCTION

A number of investigations have confirmed that about corrosion inhibition and surface passivation, the synergistic effect of multiple substances is better than the single effect of one substance [1-10], and the synergistic effect can be derived from between inorganic substances [2-4], between organic substances [5-7] as well as between organic and inorganic substances [8-10]. Al-

Refaie *et al.* [2] reported the synergistic effect between molybdate and nitrite on the surface passivation of a circular steel. Molybdate promoted the formation of both $\text{Fe}_2(\text{MoO}_4)_3$ and $\gamma\text{-Fe}_2\text{O}_3$, but nitrite only promoted the formation of $\gamma\text{-Fe}_2\text{O}_3$; the passive film composed of outer $\text{Fe}_2(\text{MoO}_4)_3$ and inner $\gamma\text{-Fe}_2\text{O}_3$ was responsible for surface passivation. Tang *et al.* [3] reported the synergistic effect between borate and phosphate on the pitting corrosion of Q235 carbon steel and 16Mn manganese steel. The synergistic effect for the 16Mn steel was better than that for the Q235 steel, resulting in the obvious positive shift of both metastable pitting potential and stable pitting potential. Zhao *et al.* [5] reported the synergistic effect between benzoate and imidazoline on the corrosion inhibition of Q235 carbon steel. The inhibition against general corrosion was mainly attributed to the adsorption of benzoate and imidazoline on the steel surface, and an adsorption model was also proposed to elucidate the synergistic effect according to zero charge potential and double layer capacitance. Zhang *et al.* [6] reported the synergistic effect between octadecylamine and tetradecyl-trimethyl-ammonium-bromide (TTAB) on the corrosion inhibition of Q235 carbon steel. The absorption of octadecylamine and TTAB was responsible for the inhibition against general corrosion at the early immersion, but at the late immersion, the former absorption was more important than the latter. Zhou *et al.* [8] reported the synergistic effect between molybdate and benzotriazole on the pitting corrosion of Q235 carbon steel. The optimal ratio of molybdate and benzotriazole was four to one, which resulted in the positive shift of pitting potential and the significant increase of inhibition efficiency. The synergistic effect was due to the transformation from FOOH to Fe_2O_3 . Zuo *et al.* [9] reported the synergistic effect between nitrite and thioureido-imidazoline on both surface passivation and pitting corrosion of X70 carbon steel. The effects of nitrite and thioureido-imidazoline were interactive and superimposed. The surface passivation was attributed to the synergistic effect, but the inhibition against pitting corrosion was closely related to the action of nitrite.

In our previous investigations [11-14], we reported the single effect and mechanism of molybdate [11], nitrite [12] and tungstate [13] on the surface passivation of Q235 carbon steel. The synergistic effect between molybdate and nitrite about corrosion inhibition [15] and surface passivation [2] for carbon steels has been reported previously; however, the published report involving the synergistic effect between molybdate and tungstate is not. It was reported that under the single action of MoO_4^{2-} or WO_4^{2-} , the critical concentrations of MoO_4^{2-} and WO_4^{2-} on the surface passivation of Q235 carbon steel are 0.08 mmol/L [11] and 0.13 mmol/L [13], respectively. Therefore, in this work, the total concentration of molybdate and tungstate is maintained at 0.20 mmol/L, and the synergistic effect between molybdate and tungstate on the surface passivation of Q235 carbon steel is investigated in mixed Na_2MoO_4 and Na_2WO_4 solutions with different ratios of MoO_4^{2-} and WO_4^{2-} by potentiodynamic polarization, Mott-Schottky and electrochemical impedance spectroscopy (EIS). Particularly, the optimal ratio of MoO_4^{2-} and WO_4^{2-} is obtained, and the related mechanism is discussed also.

2. EXPERIMENTAL

2.1 Material and solution

The investigated material was Q235 carbon steel with following chemical composition (weight

percent): C, 0.160; Mn, 0.530; Si, 0.300; S, 0.045; P, 0.015; and Fe, 98.950. A plate of Q235 carbon steel was processed into the samples with the three-dimensional size of 10 mm × 10 mm × 3 mm, and samples were manually abraded up to 1000 grit with SiC abrasive paper, rinsed with de-ionized water and degreased in alcohol.

The investigated solution was mixed Na₂MoO₄ and Na₂WO₄ solutions with different ratios of MoO₄²⁻ and WO₄²⁻. The total concentration of MoO₄²⁻ and WO₄²⁻ was maintained at 0.20 mmol/L, and five different ratios (2 to 0, 1.5 to 0.5, 1 to 1, 0.5 to 1.5 and 0 to 2) were considered. The detailed component of mixed Na₂MoO₄ and Na₂WO₄ solutions was listed in Table 1.

Table 1. Detailed component of mixed Na₂MoO₄ and Na₂WO₄ solutions with different ratios of MoO₄²⁻ and WO₄²⁻.

Solution	MoO ₄ ²⁻ (mmol/L)	WO ₄ ²⁻ (mmol/L)	pH	Name
1	0.20	0	7.0	M/W=2.0/0.0
2	0.15	0.05	7.0	M/W=1.5/0.5
3	0.10	0.10	7.0	M/W=1.0/1.0
4	0.05	0.15	7.0	M/W=0.5/1.5
5	0	0.20	7.0	M/W=0.0/2.0

2.2 Electrochemical measurement

Electrochemical measurements, including potentiodynamic polarization, Mott-Schottky and EIS, were carried out at room temperature by a CS310 electrochemical workstation. A traditional three-electrode system was used: the work electrode was a Q235 sample, the counter electrode was a platinum sheet and the reference electrode was a saturated calomel electrode (SCE). Before each electrochemical test, the work electrode was immersed in the corresponding solution for 30 min until the stability of open circuit potential (OCP). In polarization tests, the potential scanning rate was 0.5 mV/s, and the potential scanning range was from -0.5 V_{OCP} to the potential corresponding to the occurrence of transpassivation. In Mott-Schottky tests, the potential scanning rate was 5.0 mV/s, and the potential scanning range was from -0.2 V_{SCE} to 1.0 V_{SCE}. In EIS tests, a perturbation potential of 10 mV amplitude was used in the frequency range from 10⁵ to 10⁻² Hz.

3. RESULTS

3.1 Polarization test

Figure 1 shows the polarization curves of Q235 carbon steel in mixed Na₂MoO₄ and Na₂WO₄ solutions with different ratios of MoO₄²⁻ and WO₄²⁻. Under five ratios of MoO₄²⁻ and WO₄²⁻ (M/W=2.0/0.0, 1.5/0.5, 1.0/1.0, 0.5/1.5 and 0.0/2.0), the presence of obvious passive region and the absence of active-passive transition are observed on the polarization curves, indicating Q235 carbon steel exhibited the electrochemical characteristic of spontaneous passivation in mixed Na₂MoO₄ and

Na_2WO_4 solutions [16].

It is worth noting that the influence of $\text{MoO}_4^{2-}/\text{WO}_4^{2-}$ ratio on the corrosion potential (E_c) and corrosion current density (i_c) is very slight, but that on the transpassive potential (E_t) is relatively significant, implying the ratio variation of MoO_4^{2-} and WO_4^{2-} mainly affects the passivation behavior of Q235 carbon steel, rather than the corrosion behavior. Further, the polarization curves are analyzed with the Tafel fitting.

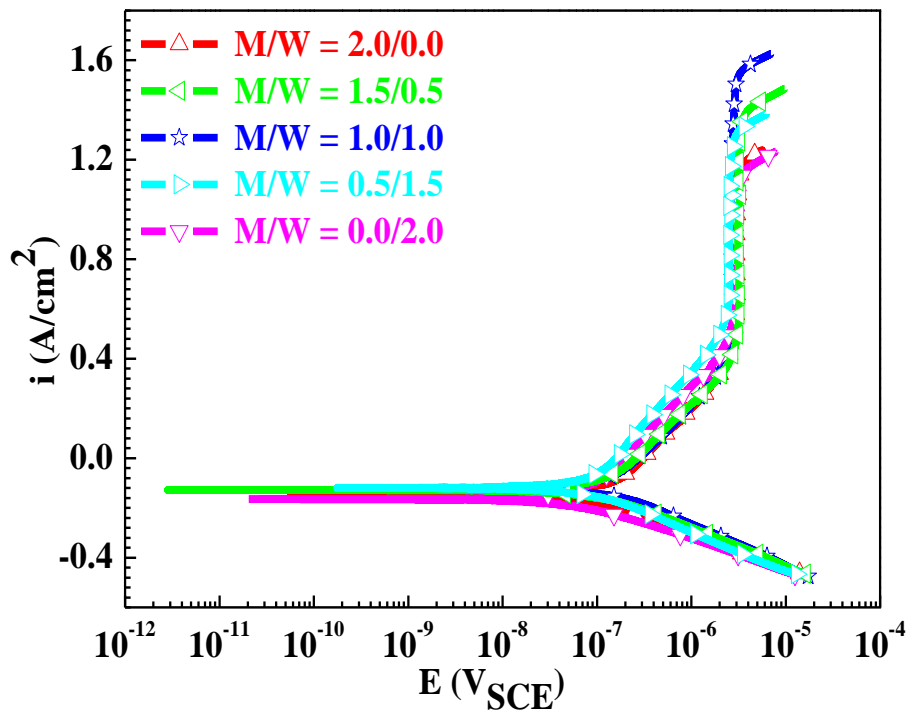


Figure 1. Polarization curves of Q235 carbon steel in mixed Na_2MoO_4 and Na_2WO_4 solutions with different ratios of MoO_4^{2-} and WO_4^{2-} .

Table 2 lists the fitted values of E_c , i_c and E_t . The values of E_c and i_c are independent of the ratio variation of MoO_4^{2-} and WO_4^{2-} , but the E_t value depends on the ratio variation. Particularly, the E_t value in the case of $M/W=1.0/1.0$ is larger than that in the other cases. Therefore, it is inferred that the optimum ratio of MoO_4^{2-} and WO_4^{2-} on the surface passivation of Q235 carbon steel is one to one.

Table 2. Fitted values of E_c , i_c and E_t of Q235 carbon steel in mixed Na_2MoO_4 and Na_2WO_4 solutions with different ratios of MoO_4^{2-} and WO_4^{2-} .

Solution	E_c (mV _{SCE})	i_c ($\mu\text{A}/\text{cm}^2$)	E_t (mV _{SCE})
M/W=2.0/0.0	-149	2.95	1153
M/W=1.5/0.5	-127	2.99	1348
M/W=1.0/1.0	-121	2.71	1545
M/W=0.5/1.5	-119	2.53	1262
M/W=0.0/2.0	-164	2.85	1089

3.2 Mott-Schottky test

Figure 2 shows the Mott-Schottky plots of Q235 carbon steel in mixed Na_2MoO_4 and Na_2WO_4 solutions with different ratios of MoO_4^{2-} and WO_4^{2-} . Under five ratios of MoO_4^{2-} and WO_4^{2-} , the slope of the straight part of Mott-Schottky plots exhibits a positive value, indicating the passive film on the surface of Q235 carbon steel formed in mixed Na_2MoO_4 and Na_2WO_4 solutions can be regarded as a n-type semiconductor [17].

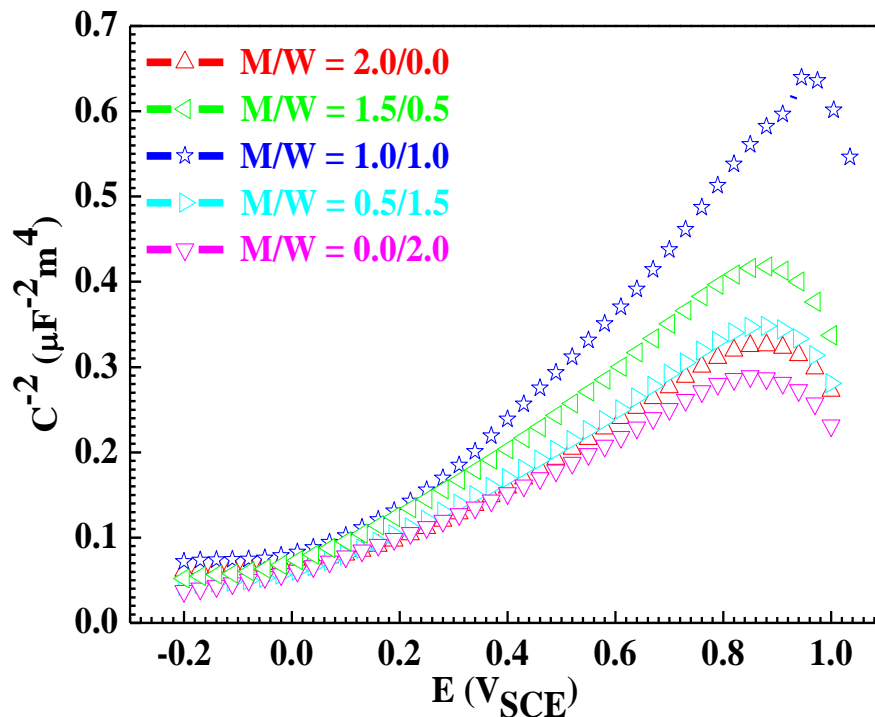


Figure 2. Mott-Schottky plots of Q235 carbon steel in mixed Na_2MoO_4 and Na_2WO_4 solutions with different ratios of MoO_4^{2-} and WO_4^{2-} .

It is generally accepted that for n-type semiconductor, its Mott-Schottky plot can be analyzed with the following equation [18]:

$$C^{-2} = 2(E - U_f - kT/e) / \epsilon \epsilon_0 e N_D \quad (1)$$

In Equation (1), C represents space charge layer capacitance, E represents applied potential, U_f represents flat band potential, k is Boltzmann constant, T is absolute temperature, e is electron charge, ϵ represents passive film permittivity, ϵ_0 is free space permittivity and N_D represents donor density. The N_D value can reflect the defect number in passive film, and the larger N_D in numerical value, the more defect in passive film [15]; the U_f value can reflect the corrosion susceptibility of metals and alloys in electrolyte solution, like the physical meaning of E_c [19].

Table 3 lists the fitted values of N_D and U_f . The ratio variation of MoO_4^{2-} and WO_4^{2-} do not affects the U_f value, which is similar to the influence of $\text{MoO}_4^{2-}/\text{WO}_4^{2-}$ ratio on E_c and i_c , confirming that the corrosion behavior of Q235 carbon steel in mixed Na_2MoO_4 and Na_2WO_4 solutions is independent of $\text{MoO}_4^{2-}/\text{WO}_4^{2-}$ ratio. The influence of $\text{MoO}_4^{2-}/\text{WO}_4^{2-}$ ratio on the N_D value is relatively

obvious, and the N_D value in the case of $M/W=1.0/1.0$ is smaller than that in the other cases. The results from Mott-Schottky test are consistent with those from polarization test, indicating that the optimum ratio of MoO_4^{2-} and WO_4^{2-} is one to one.

Table 3. Fitted values of N_D and U_f of Q235 carbon steel in mixed Na_2MoO_4 and Na_2WO_4 solutions with different ratios of MoO_4^{2-} and WO_4^{2-} .

Solution	N_D (cm^{-3})	U_f (mV_{SCE})
$M/W=2.0/0.0$	5.14×10^{18}	-134
$M/W=1.5/0.5$	3.74×10^{18}	-113
$M/W=1.0/1.0$	2.87×10^{18}	-84
$M/W=0.5/1.5$	4.27×10^{18}	-91
$M/W=0.0/2.0$	5.36×10^{18}	-121

3.3 EIS test

Figure 3 shows the EIS of Q235 carbon steel in mixed Na_2MoO_4 and Na_2WO_4 solutions with different ratios of MoO_4^{2-} and WO_4^{2-} . Under five ratios of MoO_4^{2-} and WO_4^{2-} , the presence of two capacitive semicircles and the absence of inductive semicircle are observed on the Nyquist plots, suggesting that no localized corrosion occurred on the steel surface and the passive film is intact [20]. The influence of $\text{MoO}_4^{2-}/\text{WO}_4^{2-}$ ratio on the radius of capacitive semicircle is very significant, and the capacitive radius in the case of $M/W=1.0/1.0$ is more obviously extensive than that in the other cases, further confirming the optimum ratio of MoO_4^{2-} and WO_4^{2-} .

However, two capacitive semicircles exhibited on the Nyquist plots imply that the passive film on the surface of Q235 carbon steel formed in mixed Na_2MoO_4 and Na_2WO_4 solutions may have a two-layer microstructure.

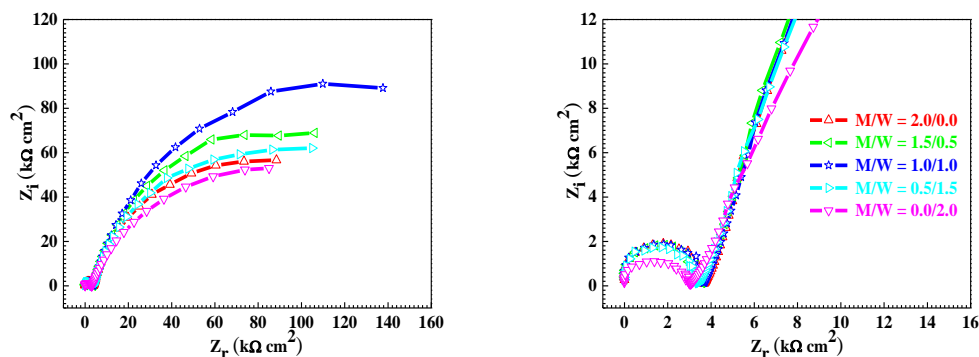


Figure 3. EIS of Q235 carbon steel in mixed Na_2MoO_4 and Na_2WO_4 solutions with different ratios of MoO_4^{2-} and WO_4^{2-} .

Further, the EIS are analyzed with equivalent electrical circuit (EEC) fitting. According to the EIS characteristic shown in Figure 3, the EEC model shown in Figure 4, which is composed of two

resistance and capacitance parallel connections, is used to analyze the EIS [21-23]. In the EEC model, R_s represents solution resistance, CPE_o and R_o respectively represent outer-layer passive film resistance and capacitance, and CPE_i and R_i respectively represent inner-layer passive film resistance and capacitance.

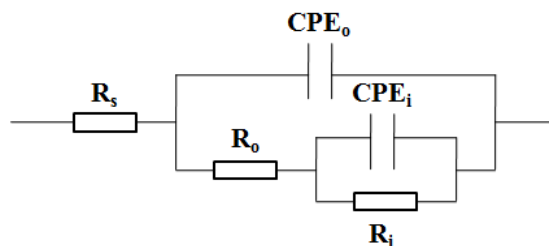


Figure 4. EEC model for EIS fitting.

Table 4 lists the fitted values of R_i and R_o . On the one hand, it is worth noting that the R_i value is independent of the ratio variation of MoO_4^{2-} and WO_4^{2-} , but the influence of MoO_4^{2-}/WO_4^{2-} ratio on the R_o value is very significant. Therefore, it is inferred that the synergistic effect between MoO_4^{2-} and WO_4^{2-} for the out-layer passive film is stronger than that for the inner-layer passive film, and the out-layer passive film may play a more important role in the surface passivation than the inner-layer passive film do. On the other hand, for the out-layer passive film, the R_o value in the case of $M/W=1.0/1.0$ is larger than that in the other cases, confirming, once again, the optimum ratio of MoO_4^{2-} and WO_4^{2-} on the surface passivation of Q235 carbon steel is one to one.

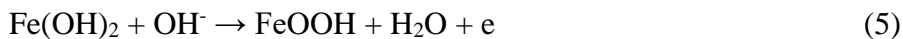
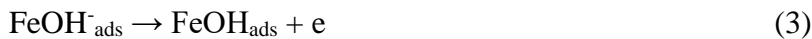
Table 4. Fitted values of R_i and R_o of Q235 carbon steel in mixed Na_2MoO_4 and Na_2WO_4 solutions with different ratios of MoO_4^{2-} and WO_4^{2-} .

Solution	R_i ($k\Omega\text{ cm}^2$)	R_o ($k\Omega\text{ cm}^2$)
M/W=2.0/0.0	3.68	84.80
M/W=1.5/0.5	3.57	102.52
M/W=1.0/1.0	3.66	134.04
M/W=0.5/1.5	3.42	101.58
M/W=0.0/2.0	3.05	81.95

4. DISCUSSION

A natural oxide film is usually formed on the surface of metals and alloys when they are exposed in air environment [24]. For carbon steels, the air-formed oxide film shows a defective and porous microstructure and do not provides anti-corrosion protection to the steel substrate [25]. However, when carbon steels serves in alkaline and neutral electrolyte environments, the air-formed oxide film can convert a two-layer passive film [26], which obeys the following reactions:





Further, FeOOH is oxidized to Fe₂O₃. The inner-layer passive film shows a compact and dense microstructure and is composed of Fe₂O₃ mainly [27], but the outer-layer passive film shows a loose and porous microstructure and is composed of Fe(OH)₂·nH₂O and Fe(OH)₃·nH₂O [28].

It was reported that under the single action of MoO₄²⁻ or WO₄²⁻, the outer-layer passive film could be repaired by the deposition of Fe₂(MoO₄)₃ [11], FeWO₄ and Fe₂(WO₄)₃ [12] at passive film defects. Therefore, it is inferred reasonably that under the synergistic action of MoO₄²⁻ and WO₄²⁻, Fe₂(MoO₄)₃, FeWO₄ and Fe₂(WO₄)₃ are in existence simultaneously in the outer-layer passive film. From the E_t, N_D and R_o values shown in Table 2, Table 3 and Table 4, on the surface passivation of Q235 carbon steel, the synergistic effect between MoO₄²⁻ and WO₄²⁻ is better than the single effect, and the optimum ratio of MoO₄²⁻ and WO₄²⁻ is one to one. At the optimum ratio, MoO₄²⁻ and WO₄²⁻ make the best to repair the defects in the outer-layer passive film.

5. CONCLUSIONS

(1) For Q235 carbon steel in mixed Na₂MoO₄ and Na₂WO₄ solutions with different ratios of MoO₄²⁻ and WO₄²⁻, the ratio variation of MoO₄²⁻ and WO₄²⁻ did not affect the corrosion behavior but affect the passivation obviously.

(2) MoO₄²⁻ and WO₄²⁻ presented the synergistic effect on the surface passivation of Q235 carbon steel, and the optimum ratio of MoO₄²⁻ and WO₄²⁻ was one to one when the total concentration was 0.2 mmol/L.

ACKNOWLEDGMENTS

The work is supported by the Middle-aged and Young University Teachers' Basic Ability Promotion Project of Guangxi (Contract 2019KY0612), the Science Research Project of High Level Talents in Yulin Normal University (Contract G2019ZK53), the National Natural Science Foundation of China (Contract 81660508) and the Guangxi Science and technology Key Research Project (Contract Guike AB17195076 and AB16380153).

References

1. X.C. Hu, P. Zhang, Y. Zhou and F.A. Yan, *Anti-Corros. Methods Mater.*, 67 (2020) 473.
2. A.A. Al-Refaie, J. Waltion, R.A. Cottis and R. Lindsay, *Corros. Sci.*, 52 (2010) 422.
3. Y.M. Tang, X.H. Zhao, J.P. Mao and Y. Zuo, *Mater. Chem. Phys.*, 116 (2009) 484.
4. X. Li, P. Zhang, H.J. Huang, X.C. Hu, Y. Zhou and F.A. Yan, *RSC Adv.*, 9 (2019) 39055.
5. J.M. Zhao and G.H. Chen, *Electrochim. Acta*, 69 (2012) 247.
6. C. Zhang and J.M. Zhao, *Corros. Sci.*, 126 (2017) 247.
7. F.G. Deng, L.S. Wang, Y. Zhou, X.H. Gong, X.P. Zhao, T. Hu and C.G. Wu, *RSC Adv.*, 7 (2017) 48876.
8. Y. Zhou, Y. Zuo and B. Lin, *Mater. Chem. Phys.*, 192 (2017) 86.

9. Y. Zuo, L. Yang, Y.J. Tan, Y.S. Wang and J.M. Zhao, *Corros. Sci.*, 120 (2017) 99.
10. Q.Y. Xiong, Y. Zhou and J.P. Xiong, *Int. J. Electrochem. Sci.*, 10 (2015) 8454.
11. P. Zhang, Y.J. Chen, H.J. Huang, Y. Zhou, F.A. Yan and G.C. Nie, *Surf. Rev. Lett.*, 27 (2020) 1950179.
12. Y. Zhou, H.J. Huang, P. Zhang, D. Liu and F.A. Yan, *Surf. Rev. Lett.*, 26 (2019) 1850218.
13. Y.J. Chen, P. Zhang, Y. Zhou and F.A. Yan, *Anti-Corros. Methods Mater.*, 67 (2020) 483.
14. Y. Zhou, P. Zhang, H.J. Huang, J.P. Xiong and F.A. Yan, *J. Braz. Chem. Soc.*, 30 (2019) 1688.
15. Y. Zhou and Y. Zuo, *Appl. Surf. Sci.*, 353 (2015) 924.
16. Y. Zhou and F.A. Yan, *Int. J. Electrochem. Sci.*, 11 (2016) 3976.
17. X. Chen, Q.Y. Xiong, F. Zhu, H. Li, D. Liu, J.P. Xiong and Y. Zhou, *Int. J. Electrochem. Sci.*, 13 (2018) 1656.
18. L.C. Chen, P. Zhang, Q.Y. Xiong, P. Zhao, J.P. Xiong and Y. Zhou, *Int. J. Electrochem. Sci.*, 14 (2019) 919.
19. J. Yang, P. Zhang, Y. Zhou and F.A. Yan, *Int. J. Electrochem. Sci.*, 14 (2019) 11349.
20. R.J. Deng, P. Zhang, X.Y. Zhao, G.Y. Cai, H. Li, J.P. Xiong and Y. Zhou, *J. Braz. Chem. Soc.*, 31 (2020) 731.
21. Y. Zhou, J.P. Xiong and F.A. Yan, *Surf. Coat. Technol.*, 328 (2017) 335.
22. Q.Y. Xiong, J.P. Xiong, Y. Zhou and F.A. Yan, *Int. J. Electrochem. Sci.*, 12 (2017) 4238.
23. Y. Zhou, P. Zhang and F.A. Yan, *Mater. Lett.*, 284 (2021) 128930.
24. Y. Zhou, P. Zhang, J.P. Xiong and F.A. Yan, *Anti-Corros. Methods Mater.*, 66 (2019) 879.
25. Y. Zhou, P. Zhang, Y. Zuo, D. Liu and F.A. Yan, *J. Braz. Chem. Soc.*, 28 (2017) 2490.
26. M.B. Valcarce and M. Vazquez, *Electrochim. Acta*, 53 (2008) 5007.
27. D.Y. Lee, W.C. Kim and J.G. Kim, *Corros. Sci.*, 64 (2012) 105.
28. F.R. Foulkes and P. McGrath, *Cem. Concr. Res.*, 29 (1999) 873.
29. Y. Zhou, P. Zhang, J.P. Xiong and F.A. Yan, *RSC Adv.*, 9 (2019) 23589.